COMPUTER SCIENCES DEPARTMENT

University of Wisconsin-Madison

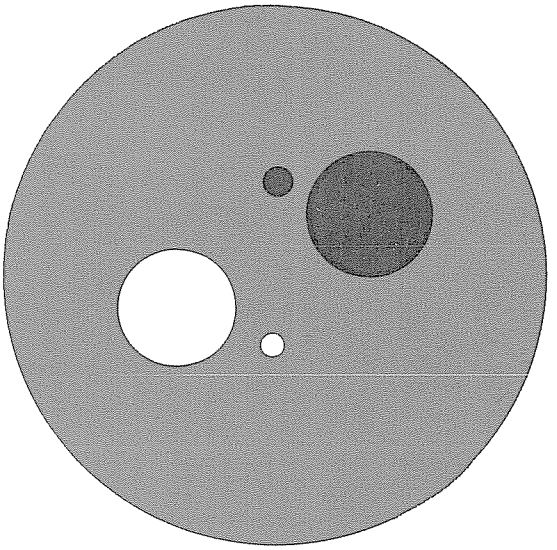

A PARTICLE MODEL OF THE STEFAN PROBLEM

by

Donald Greenspan

Computer Sciences Technical Report #281

DECEMBER 1976

Abstract

The melting of triangular and rectangular solids is analyzed by means of new particle-type models. Heating is defined in terms of the increase of a particle's velocity, while temperature is defined in terms of a particle's kinetic energy. Computer examples are given of slow heating, fast heating, heating from above and heating from below. In each case the liquid and the solid portions are clearly delineated.

1. Introduction

Stefan problems are free boundary problems associated with the processes of melting of solids and crystallizing of liquids. The name is derived from one of the early studies of Arctic ice formation [15]. Specifically, the problem is that of describing the changing shape of the boundary between the liquid portion and solid portion when either, or both, of the above processes are occurring.

The Stefan problem is of such difficulty that classical mathematical studies have been restricted largely to existence, uniqueness, and asymptotic behavior of a one dimensional model based on the linear heat equation (see, e.g., [7], [11], [14] and the numerous references contained therein). The recent availability of high speed digital computation has led to the development of finite difference, variational, finite element, and Chebyshev-series numerical methods for approximating the solution of the problem (see, e.g., [2], [4]-[6], [10], [13], and the numerous additional references contained therein). Most of these methods have been applied to one dimensional problems only, and, in all cases, only to the linear heat equation. Indirect efforts, which avoid computing the free boundary, itself, have also been developed and require either the numerical solution of a nonlinear partial differential equation ([3], [12]) or the numerical solution of a variational inequality [1].

In this paper we will develop still another numerical approach to Stefan problems. Though attention will be restricted to the melting phenomenon only, it is equally applicable to crystallization. In the spirit which von Neuman [16] recommended for the study of shock wave development in gases, we will construct particle type solids which are bonded by molecular type forces and then melt these directly.

2. Basic Definitions and Formulas

For positive time step Δt, let $t_k = k\Delta t$, $k = 0,1,2,\ldots$. For $i = 1,2,\ldots,N$, let particle P_i have mass m_i and at time t_k let P_i be located at $\vec{r}_{i,k} = (x_{i,k},y_{i,k})$, have velocity $\vec{v}_{i,k} = (v_{i,k,x}, v_{i,k,y})$, and have acceleration $\vec{a}_{i,k} = (a_{i,k,x},a_{i,k,y})$. Let position, velocity and acceleration be related by the "leap-frog" formulas [8], p. 107):

$$\vec{v}_{i,\frac{1}{2}} = \vec{v}_{i,0} + \frac{\Delta t}{2}\vec{a}_{i,0} \tag{2.1}$$

$$\vec{v}_{i,k+\frac{1}{2}} = \vec{v}_{i,k-\frac{1}{2}} + (\Delta t)\vec{a}_{i,k} , \qquad k = 1,2,\ldots \tag{2.2}$$

$$\vec{r}_{i,k+1} = \vec{r}_{i,k} + (\Delta t)\vec{v}_{i,k+\frac{1}{2}} , \qquad k = 0,1,2,\ldots . \tag{2.3}$$

If $\vec{F}_{i,k}$ is the force acting an P_i at time t_k , where $\vec{F}_{i,k} = (F_{i,k,x},F_{i,k,y})$, then we assume that force and acceleration are related by

$$\vec{F}_{i,k} = m_i \vec{a}_{i,k} . \tag{2.4}$$

Once an exact structure is given to $\vec{F}_{i,k}$, the motion of each particle will be determined recursively and explicitly by (2.1)-(2.4) from prescribed initial data. The special structure to be used is described as follows.

At time t_k , let $r_{ij,k}$ be the distance between P_i and P_j . Let G (coefficient of attraction), H (coefficient of repulsion),

β (exponent of attraction) and α (exponent of repulsion) be determined subject to the constraints $G \geq 0$, $H \geq 0$, $\alpha \geq \beta \geq 2$ (see [8]). Then the force $(F_{i,k,x},F_{i,k,y})$ exerted on P_i by P_j is given by

$$F_{i,k,x} = \left[\frac{-G\, m_i\, m_j}{r_{ij,k}^{\beta}} + \frac{H\, m_i\, m_j}{r_{ij,k}^{\alpha}}\right]\frac{x_{i,k}-x_{j,k}}{r_{ij,k}} \tag{2.5}$$

$$F_{i,k,y} = \left[\frac{-G\, m_i\, m_j}{r_{ij,k}^{\beta}} + \frac{H\, m_i\, m_j}{r_{ij,k}^{\alpha}}\right]\frac{y_{i,k}-y_{j,k}}{r_{ij,k}} . \tag{2.6}$$

The total force $(F^*_{i,k,x}, F^*_{i,k,y})$ on P_i due to all the other N-1 particles is given by

$$F^*_{i,k,x} = \sum_{\substack{j=1 \\ j\neq i}}^{N} F_{i,k,x};\quad F^*_{i,k,y} = \sum_{\substack{j=1 \\ j\neq i}}^{N} F_{i,k,y} . \tag{2.7}$$

Finally, we include gravity into the model by setting

$$F_{i,k,x} = F^*_{i,k,x};\quad F_{i,k,y} = F^*_{i,k,y} - 32m_i . \tag{2.8}$$

The formulation (2.1)-(2.8) is explicit and economical, though nonconservative. Conservation of energy and momenta can be achieved [8], but only through an implicit, less economical approach.

In all calculations to be described, the time step will be $\Delta t = 0.0001$ and the FORTRAN program used is that in the Appendix of [9].

3. Examples of Particle Solids

A particle solid is a system of particles in which the attraction-repulsion force components are more significant than the force of gravity, thus resulting in interparticle bonding. Since the generation of such solids is of exceptional mathematical difficulty, they are usually generated by computer techniques. Two such solids generated recently [9] will be described next.

For $N = 28$, let $m_i \equiv 1$, $G = 2500$, $H = 2900$, $\alpha = 6$, and $\beta = 4$. We will consider a triangular body first and assume that it is supported by the X-axis, which is implemented as follows. If any particle P_i falls below the X-axis at times t_k, then its position is reflected and its velocity damped as follows:

$$(3.1) \qquad x_{i,k} \to x_{i,k},\ y_{i,k} \to -y_{i,k},\ v_{i,k,x} \to 0,\ v_{i,k,y} \to (-0.1)\, v_{i,k,y}.$$

Moreover, in order to assure that the effects of $\bar{F}_{i,k,x}$ and $\bar{F}_{i,k,y}$ in (2.5)-(2.6) are local, these forces will be set equal to zero whenever $|P_iP_j| > 1.5$. Then, a triangular particle solid generated in accordance with the above constraints is shown in Figure 3.1 and its particles' positions and velocities are given in Table 1. These positions and velocities will be the initial data of all computations to be considered in the next section.

We will consider also the following rectangular particle solid. For $N = 46$, let $m_i \equiv 1$, $G = 2540$, $H = 2940$, $\alpha = 10$, $\beta = 7$. All other parameters and constants are the same as for the triangular solid.

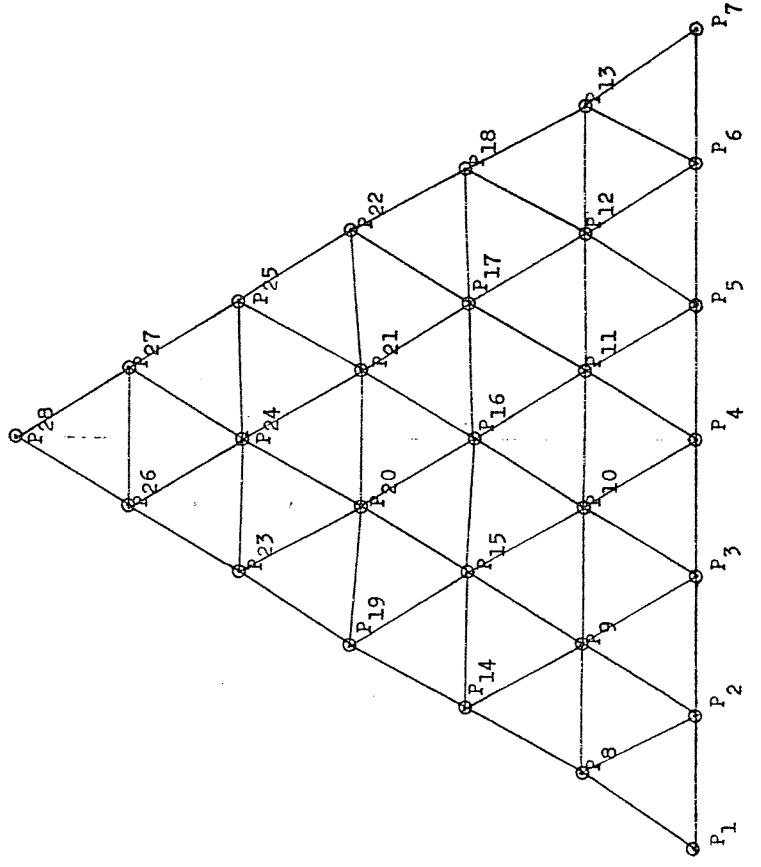

FIGURE 3.1

TABLE 1 - Equilibrium Positions and Velocities of Particles P_i : Triangular Body

i	x	y	v_x	v_y
1	-3.2652	0.0000	0.0000	0.0005
2	-2.1924	0.0000	0.0000	0.0065
3	-1.0895	0.0000	0.0000	0.0018
4	0.0000	0.0000	0.0000	0.0016
5	1.0895	0.0000	0.0000	0.0018
6	2.1924	0.0000	0.0000	0.0065
7	3.2652	0.0000	0.0000	0.0005
8	-2.6754	0.8909	-0.9437	1.0055
9	-1.6310	0.8990	2.0010	3.7973
10	-.5445	0.9032	4.1844	-0.9128
11	.5445	0.9032	-4.1844	-0.9128
12	1.6310	0.8990	-2.0010	3.7973
13	2.6754	0.8909	0.9437	1.0055
14	-2.1366	1.8374	0.9267	0.4191
15	-1.0763	1.8146	-2.5412	-2.1506
16	0.0000	1.7923	0.0000	-1.5731
17	1.0763	1.8146	2.5412	-2.1506
18	2.1366	1.8374	-0.9267	0.4191
19	-1.6674	2.7530	-0.9468	0.6165
20	-0.5441	2.6879	-1.8075	2.1719
21	0.5441	2.6879	1.8075	2.1719
22	1.6674	2.7530	0.9468	0.6165
23	-1.0877	3.6478	0.2061	-2.6777
24	0.0000	3.6174	0.0000	0.4901
25	1.0877	3.6478	-0.2061	-2.6777
26	-0.5536	4.5068	-0.5620	0.7410
27	0.5536	4.5068	0.5620	0.7410
28	0.0000	5.4351	0.0000	-2.8452

Then the solid so generated [9] is shown in Figure 3.2 and its particle positions and velocities are given in Table 2. These positions and velocities will be the initial data for all computations to be described in Section 5.

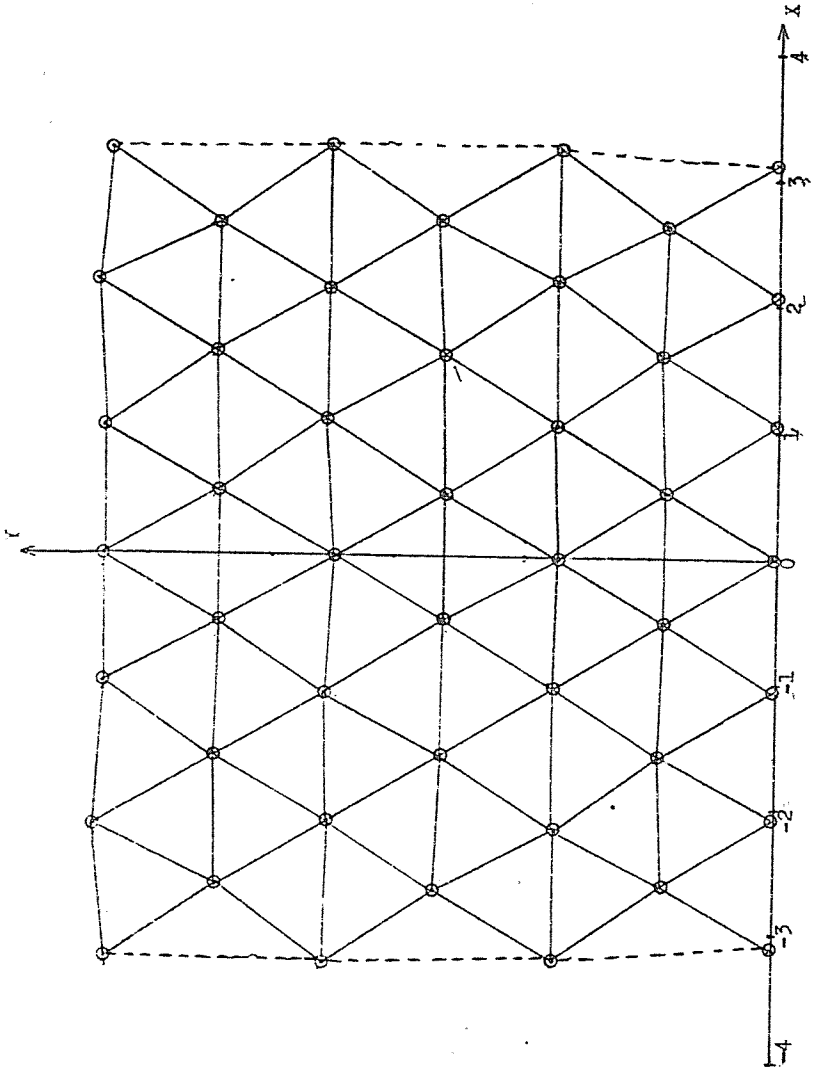

FIGURE 3.2

TABLE 2 - Equilibrium Positions and Velocities of Particles P_i : Rectangular ody

i	x	y	v_x	v_y
1	-3.1286	0.0000	-.0064	-.0143
2	-2.0758	0.0000	-.0027	.0000
3	-1.0569	0.0000	.0025	.0000
4	0.0000	0.0000	.0000	-.0379
5	1.0569	0.0000	-.0025	.0000
6	2.0758	0.0000	.0027	.0000
7	3.1286	0.0000	.0064	-.0143
8	-2.6141	.8925	1.9772	-2.5275
9	-1.5702	.9063	-.2578	-1.6351
10	-.5158	.8806	-.4572	-4.0032
11	.5158	.8806	.4572	-4.0032
12	1.5702	.9063	.2578	-1.6351
13	2.6141	.8925	-1.9772	-2.5275
14	-3.2355	1.7328	.1082	.3596
15	-2.1869	1.7561	-3.4152	1.9154
16	-1.0613	1.7556	4.0996	1.9352
17	.0000	1.7118	.0000	-3.1557
18	1.0663	1.7556	-4.0996	1.9352
19	2.1869	1.7561	3.4152	1.9154
20	3.2355	1.7328	-.1082	.3596
21	-2.6612	2.6948	6.7863	2.4723
22	-1.6000	2.6242	-.9479	-.7837
23	-.4951	2.6327	1.5791	.2733
24	.4951	2.6327	-1.5791	.2733
25	1.6000	2.6242	.9479	-.7837
26	2.6612	2.6946	-6.7858	2.4723
27	-3.2632	3.5724	6.3615	1.2408
28	-2.1325	3.5437	-.1162	.8118
29	-1.1082	3.5822	-.5865	-.9931
30	.0000	3.4975	.0000	2.1883
31	1.1082	3.5822	.5865	-.9931
32	2.1325	3.5437	.1162	.8118
33	3.2632	3.5724	-6.3615	1.2408
34	-2.6332	4.4355	.1184	-2.9408
35	-1.6157	4.4688	-6.3966	-1.1250
36	-.5082	4.4248	-.7457	2.3525
37	.5082	4.4248	.7457	2.3525
38	1.6157	4.4688	6.3956	-1.1250
39	2.6332	4.4355	-.1184	-2.9408
40	-3.2233	5.3069	3.3095	-5.0351
41	-2.1720	5.4220	.6164	-3.5662
42	-1.0380	5.3376	.0952	-1.2303
43	.0000	5.3734	.0000	1.7940
44	1.0380	5.3376	-.0952	-1.2303
45	2.1720	5.4220	-.6164	-3.5632
46	3.2233	5.3069	-3.3095	-5.0351

4. Melting of a Triangular Solid

Consider first the triangular particle solid shown in Figure 3.1 and let us consider the effect of placing a heat source near, but to the right, of the uppermost particle P_{28}, say, at (0.2, 5.7). Heat will be transferred to the body by increasing the velocity, and hence the kinetic energy, of various body particles as follows. At each time step t_k, consider the distance R_i of particle P_i to the heat source. If $R_i \geq 2.5$, then P_i's velocity is left unchanged. If $R < 2.5$, then its velocity components are reset to

$$(4.1) \qquad \vec{v}_{i,k} = \left(v_{i,k,x} + \frac{\Gamma}{R_i^2}\,\frac{(x_{i,k}-0.2)}{R_i},\ v_{i,k,y} + \frac{\Gamma}{R_i^2}\,\frac{(y_{i,k}-5.7)}{R_i}\right),$$

so that the intensity varies as an inverse square, with Γ being a positive variation constant, and along the line joining the center of the particle and the center of the heat source. In order to simulate a gradual increase of heat at the source, itself, Γ is increased with time in the following fashion. Particle motions are calculated with $\Gamma = 0.008$ for 50000 time steps, then with $\Gamma = .0095$ for 30000 additional time steps, and finally with $\Gamma = 0.015$ for 20000 time steps. The total physical time of the 100000 time steps is 10 seconds.

The question of whether or not a particle is a fluid particle or a solid particle can be determined in two ways. Both involve the observation from the computations of the first breaking of a bonded triple of particles. One method uses only the critical speeds involved, and

will be applied in this section. The second method uses the concept of critical temperature and will be applied in the next section. Hence, for the triangular solid of Figure 3.1, the distance between any two particles in a triangular bond of three particles never exceeds 1.5, since $\vec{F}^* \equiv \vec{0}$ if $r_{ij,k} > 1.5$. In addition, if one defines the average linear velocity $v^*_{i,k}$ of P_i at t_k by

$$(4.2) \qquad v^*_{i,k} = \frac{\vec{v}_{i,k} - \vec{v}_{i,k-1000}}{0.1},$$

which is a measure of the gross motion of the particle, then $v^*_{i,k} > 7.5$ invariably seems to yield the breaking of a three-particle bond. Thus, we define a particle P_i at t_k to be a solid particle if both the following are valid:

(a) P_i and two other particles are vertices of a triangle for which each side has length less than 1.5,

(b) $|v^*_{j,k}| \leq 7.5$ for each particle of the triangle in (a).

Otherwise, P_i is said to be a fluid particle.

Using the above criteria, Figure 4.1 shows the melting of the triangular solid from t_{80000}-t_{100000}. The boundary between the solid and liquid portion is delineated by drawing line segments between all solid particles which are separated by a distance less than 1.5 units. Fluid particles with average speeds greater than 7.5 units have directional arrows attached, while those with velocities less than 7.5 do not.

Figure 4.1 (a) shows the slight deformation of the solid at t_{80000}

due to the accumulation of heat, while (b) shows a more rapid and more intensive deformation by the time t_{82000}. Melting appears in Figure 4.1 (c) at t_{84000} and accumulates to a flow down the left side by the time t_{86000}, as shown in (d). Figure 4.1 (e), at t_{87000}, shows that P_1 has moved to the left sufficiently to enable P_{19} to bond with P_1 and P_8. However, the direction of P_{28} suggests that this bond cannot endure. In addition, as the particles in the upper right hand section of the solid begin to regroup, P_{25} has converted its potential energy into kinetic energy and has become a fluid particle. At this time, t_{87000}, no particle is receiving any heat from the source because all particles are now at least 2.25 units from the source. If figure (f), at t_{88000}, one sees three interesting formations. First, the bond which P_{19} has formed with P_1 and P_8 is beginning to break. Second, the bottom row has buckled, as was beginning to be evident in figure (e), a phenomenon which results from the limitation of horizontal motion inherent in (3.1). Third, particles P_{17}, P_{22}, P_{21}, P_{27} and P_{16}, though each a solid particle, are also particles which surround a relative void. Mutual attraction must then lead to a collapse into the void and the formation of additional bonds. In figure (g) at t_{94000} we see that P_{19} has formed a new bond with P_1 and P_{28}, while P_{17}, P_{22}, P_{21}, P_{27} and P_{16} have formed additional bonds, as predicted, but thereby leaving P_{25} unbonded, and hence a fluid particle. P_{25} then falls under the motion of gravity until it rebonds with P_{13} and P_{18}, as shown in figure (h) at t_{100000}, which is the final equilibrium formation. Only P_{23} remains as a fluid particle.

FIGURE 4.1

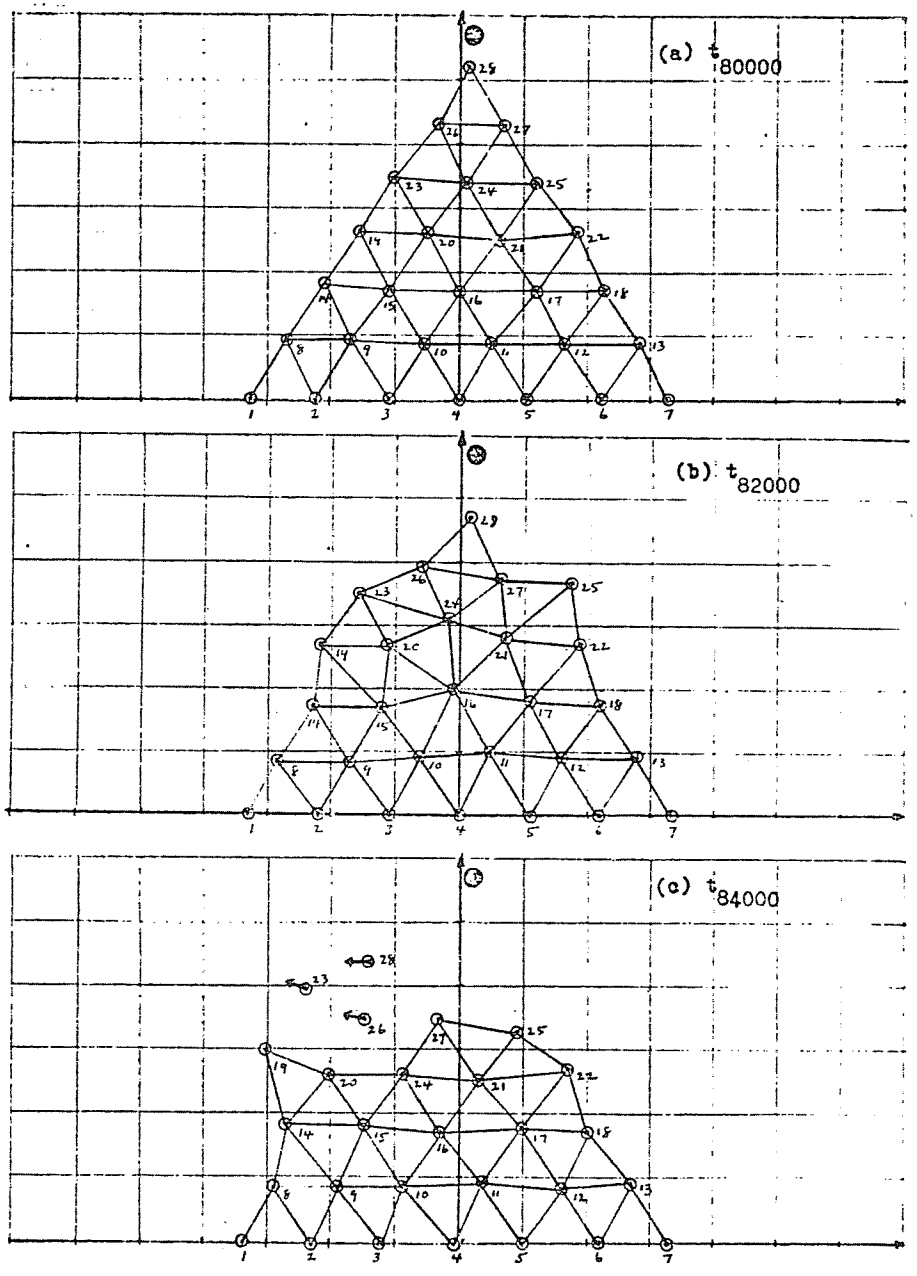

FIGURE 4.1 - continued

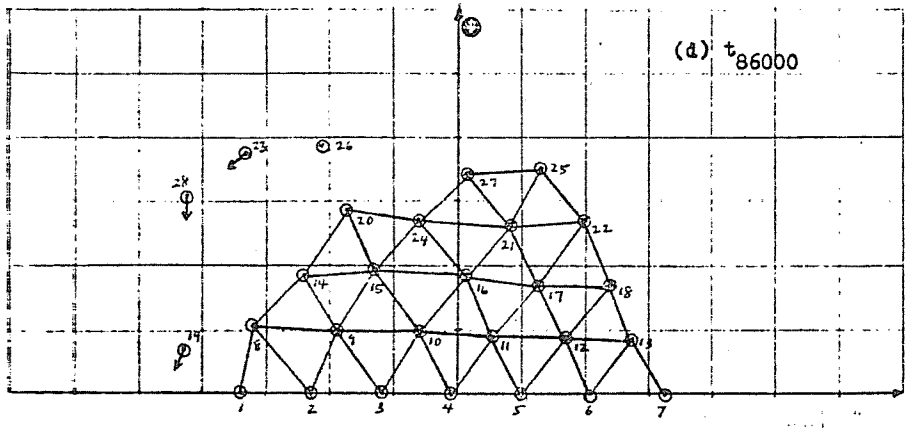

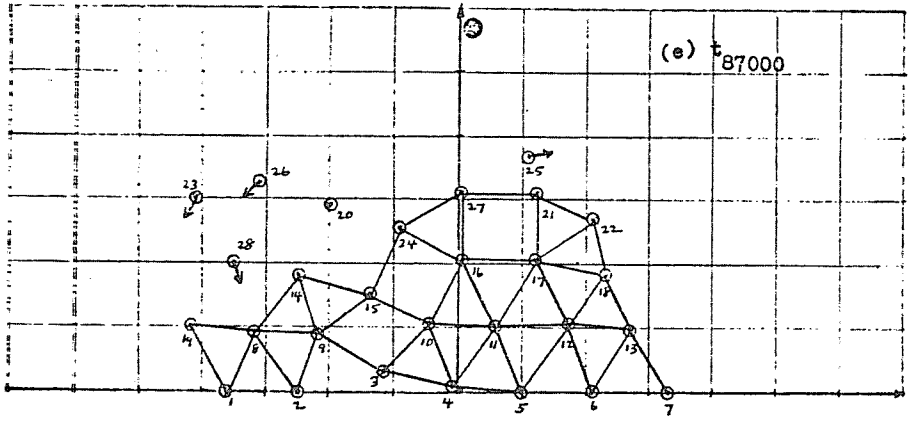

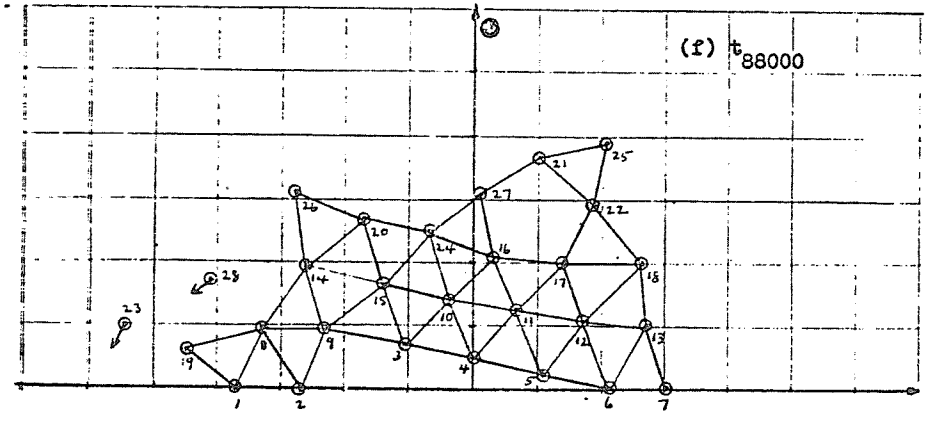

FIGURE 4.1 - continued

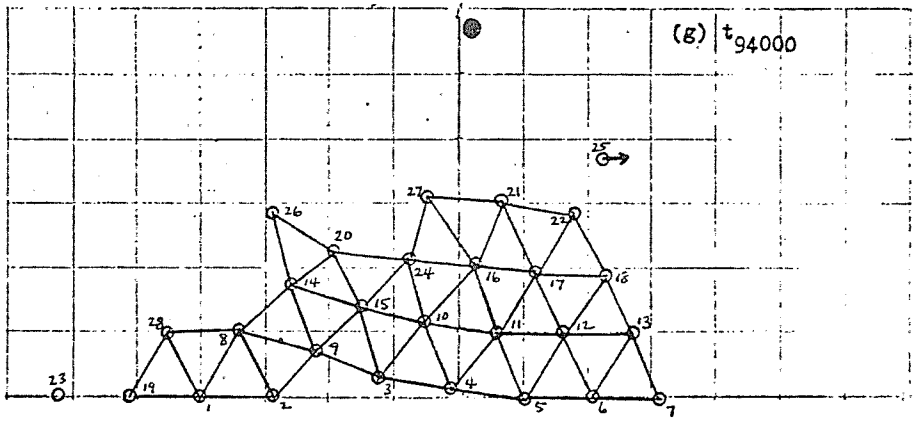

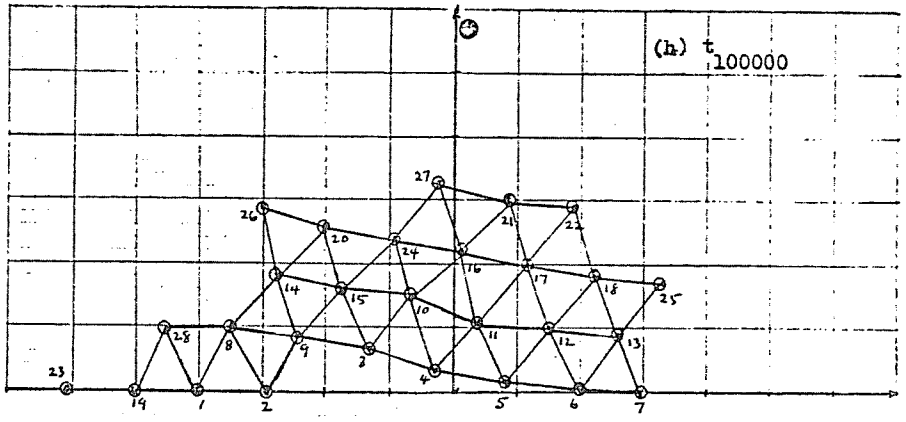

The melting and resolidifying processes in this example resemble the melting of a wax-like solid.

A more intensive type of heating is shown in Figure 4.2. In this example, the heat source at (0.2, 5.8) is applied with $\Gamma = 0.02$ immediately and a splashing, or splattering, effect results quickly. Figure (c) is especially revealing of this motion. In (e), at t_{5000}, the main body is resolidifying, buckling is becoming apparent in the base, and liquid particles are falling to the left and the right of the main body. Interestingly enough, by t_{30000}, as shown in (g), an equilibrium has been reached in which all particles have returned to the solid state. The solidification of P_{19}, P_{20} and P_{23} is a result of interparticle attraction and of the heat conduction capacity of the base, inherent in (3.1).

FIGURE 4.2

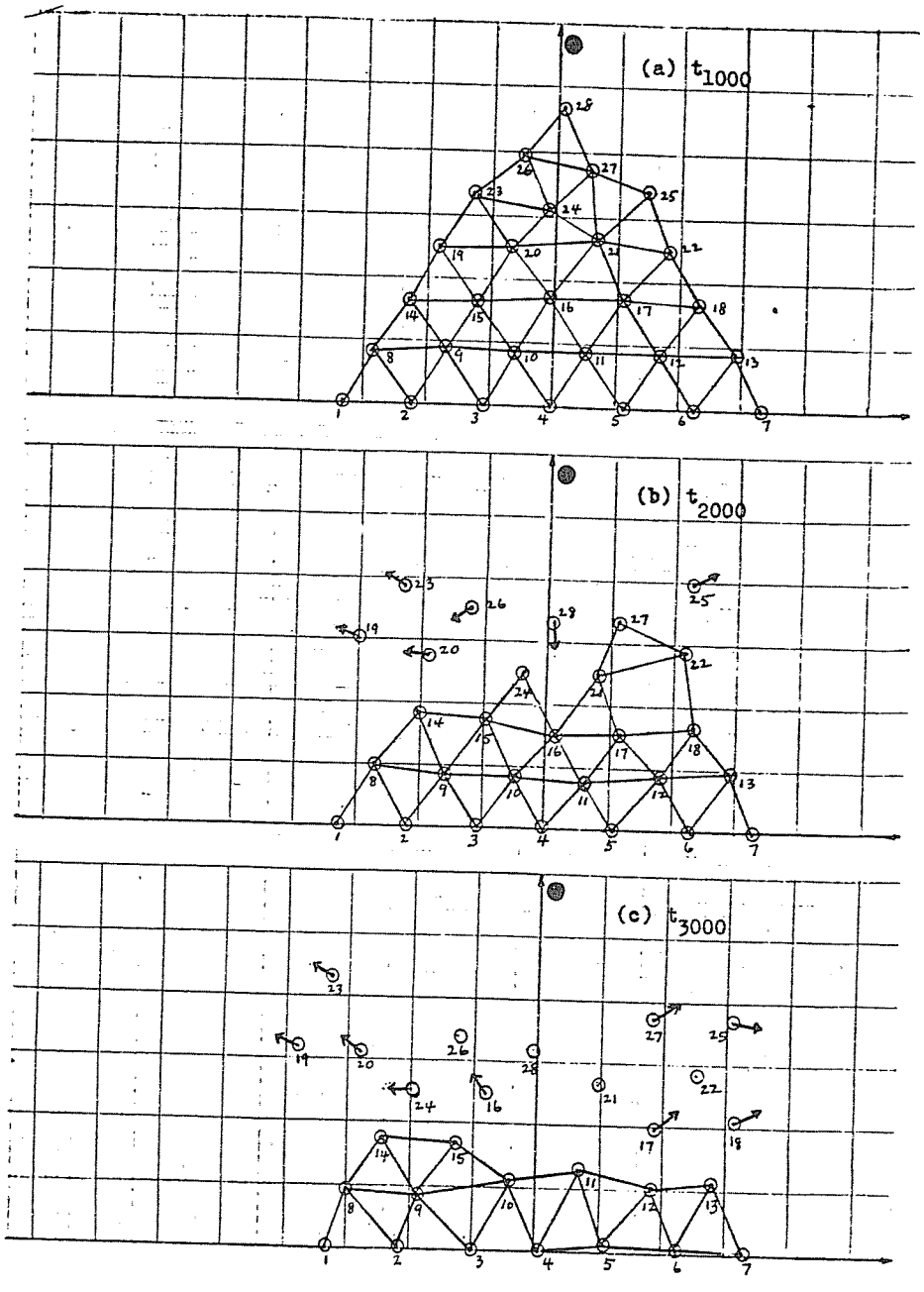

FIGURE 4.2 - continued

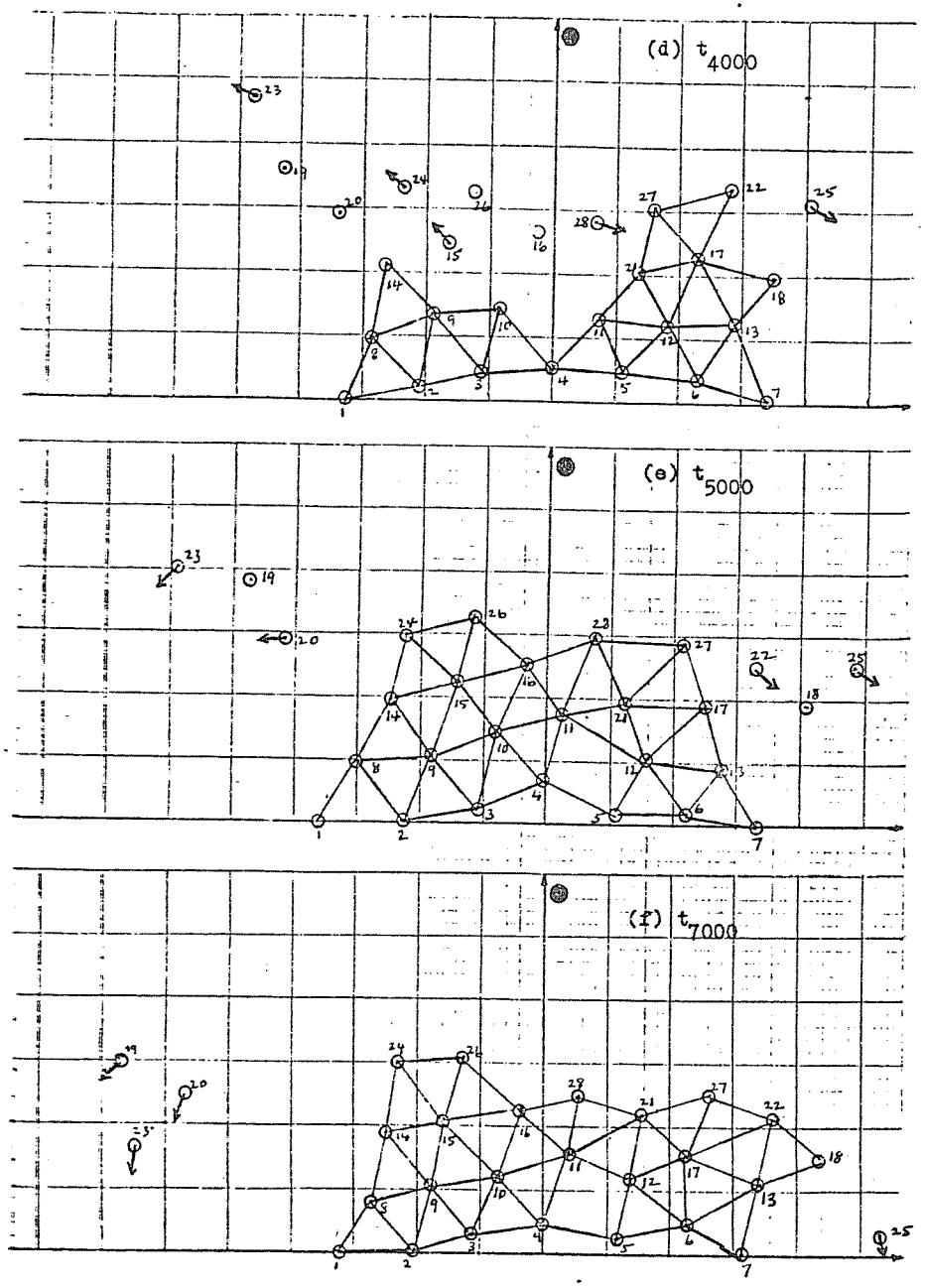

FIGURE 4.2 - continued

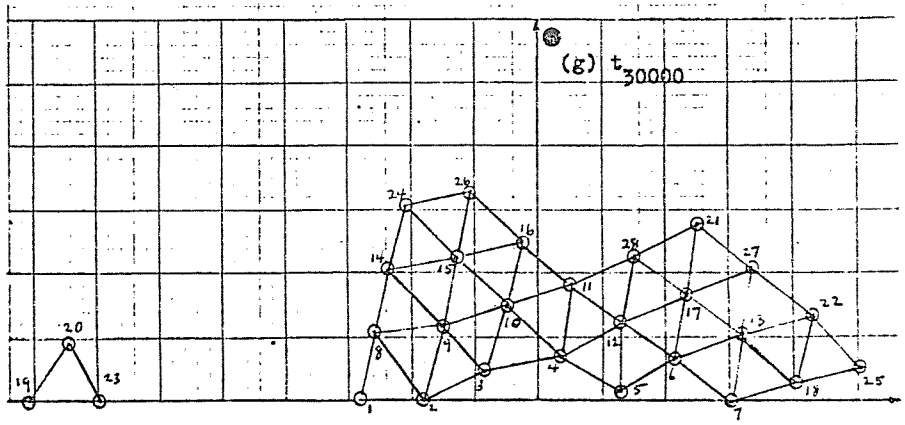

5. Melting of a Rectangular Solid

Consider now the rectangular solid shown in Figure 3.2 and consider heating it along the bottom. To do this, we merely change the reflection rule (3.1) as follows.

$$v_{i,k,y} \to (-\gamma)v_{i,k,y}, \ \gamma > 0 \ ,$$

where γ is a measure of the heat in the base. In particular, let us choose γ as follows:

$$(5.1) \quad \begin{cases} \gamma = 0.1 & , \ |x| \geq 5 \\ \gamma = 1.5 - (0.025)(x+5) & , \ -5 < x < 5 \ , \end{cases}$$

thus yielding strong, slightly asymmetrical heating only in the interval $-5 < x < 5$.

As indicated in Section 4, we will describe the melting process this time by introducing the concept of temperature [8]. The temperature $T_{i,k}$ of P_i at t_k is defined to be the arithmetic mean of P_i's kinetic energies over the time steps $t_1, t_2, \ldots, t_k$. Using this definition, computations reveal that the two particles in the lower left and lower right hand corners of Figure 3.2 break their bonds when their temperatures reach $T = 25$. Thus, we differentiate between fluid and solid particles as follows. A particle P_i and t_k is said to be a solid particle if both the following are valid:

(a) P_i and two other particles are vertices of a triangle for

which each side has length less than 1.5;

(b) $T_{j,k} < 25$ for each particle of the triangle in (a).

Otherwise, P_i is said to be a fluid particle.

Using these criteria, Figure 5.2 shows the melting of the solid through t_{50000}, at which time all the particles are fluid particles and are flowing outward in two distinct, wavelike portions. The solid particles are, as in Section 4, shown by means of connecting segments, and the gradual dissipation of the solid bulk is clearly revealed in figures (a)-(d). Figure (b) also reveals of collapse of a solid section above a portion of fluid.

FIGURE 5.2

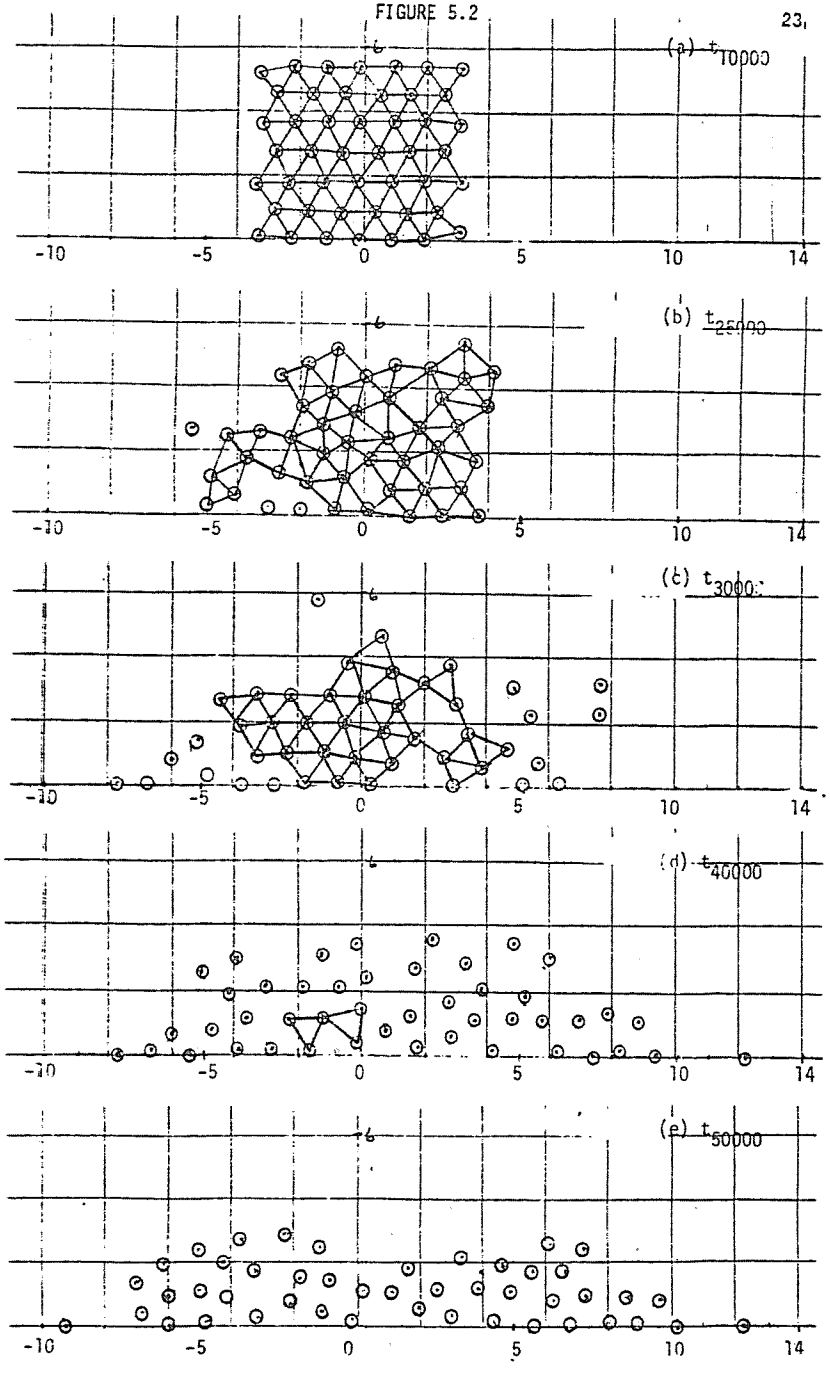

6. Remarks

From the large variety of computations with other parameter choices, it was found that, both physically and computationally, the triangular solid was more acceptable than the rectangular one. The basic reason was not one of shape, but of the choices of α and β, the exponents of attraction and repulsion. One should expect each particle in a particle solid to behave like an aggregate of molecules, and not like individual molecules themselves. The α and β choices for the rectangular solid are much closer to realistic exponents for actual molecules than are those for the triangular solid. Thus, small relative changes, like the selection of $\gamma = 2.5$ on $-5 \le x \le 5$ in (5.1), led to exceptionally large forces and volatile computational results. Comparably small changes in Γ in (4.1) led to relatively reasonable results.

In addition, the use of temperature rather than average velocity in determining the solid or fluid state of a particle proved to be more practical and physically appealing. The choice of time span in (4.2), or, more generally, the choice of M in

$$v^*_{i,k} = \frac{\vec{v}_{i,k} - \vec{v}_{i,k-M}}{M\Delta t} ,$$

is often a most difficult choice, because a single M is not always adequate throughout the system. On the other hand, the temperature test used in Section 5 can be applied easily, a priori, along the base of any given solid to determine the critical temperature, which can then be utilized in subsequent heating problems. Moreover, of the

two methods, the temperature approach is more consistent with the concepts of statistical mechanics.

Finally, it should be noted that computations with much larger solids is now in the planning stage. Of special interest will be melting due to radiant heat, which will be implemented by the introduction of shadow regions [8], so that only exposed portions of the solid will be heated. The programs and computations will, of necessity, be much more extensive than those of this paper.

References

1. J. Aguire-Puente and M. Fremond, "Frost propagation in wet porous media", Proceedings of Joint IuTAM/IMU Symposium on Application of Methods of Functional Analysis to Problems of Mechanics (Marseille, 1975), Springer-Verlag, 1976.

2. R. Bonnerot and P. Jamet, "A second order finite element method for the one-dimensional Stefan problem", Int. Jour. Num. Meth. Engg., 8, 1974, pp 811-820.

3. J. F. Ciavaldini, "Analyse numerique d'un probleme de Stefan", SIAM Jour. Num. Anal., 12, 1975, pp 464-487.

4. J. Crank, "Two methods for the numerical solution of moving-boundary problems in diffusion and heat flow", QJMAM, 10, 1957, pp 220-231.

5. J. Douglas and T. M. Gallie, "On the numerical integration of a parabolic differential equation subject to a moving boundary condition", Duke Math. Jour.,122, 1955, pp 557-571.

6. L. W. Ehrlich, "A numerical method of solving a heat flow problem with moving boundary", Jour. ACM, 5, 1958, pp 161-176.

7. A. Friedman, Partial Differential Equations of Parabolic Type, Prentice-Hall, Englewood Cliffs, N.J., 1964.

8. D. Greenspan, Discrete Models, Addison-Wesley, Reading, Mass., 1973.

9. D. Greenspan and M. Rosati, "Computer generation of particle solids", TR273, Comp. Sci. Dept., U. of Wisconsin, Madison, 1976.

10. P. Jamet and R. Bonnerot, "Numerical computation of the free boundary for the two-dimensional Stefan problem by finite elements", Centre d'Etudes de Limeil, Service M.A., B.P. 27, 94190 Villeneuve-St-Georges, France.

11. C. Li-Shang, "Existence and differentiability of the solution of a two-phase Stefan problem for quasilinear parabolic equations", Chinese Math.,7, 1965, pp 481-496.

12. G. H. Meyer, "Multidimensional Stefan problems", SIAM Jour. Num. Anal., 10, 1973, pp 522-538.

13. O. Osterby, "Analysis of numerical solution of the Stefan problem", DAIMI PB-24, Dept. Comp. Sci., Univ. Aarhus, 1974.

14. L. Rubinsteins, The Stefan Problem (in Russian), Latvian State University Computing Center, Izdat. "Zvaigzne", Riga, 1967.

15. J. Stefan, "Uber die Theorie der Eisbildung, insbesondere uber die Eisbildung im Polarmeere", Sitz. Akad. Wiss. Wien, Mat.-Nat. Classe, 98, 1889, pp 965-983.

16. J. von Neumann, "Proposal and analysis of a new numerical method for the treatment of hydrodynamical shock problems", in The Collected Works of John von Neumann, vol. 6, No. 27, Pergamon, N.J., 1963.